Nanoscale

Accepted Manuscript

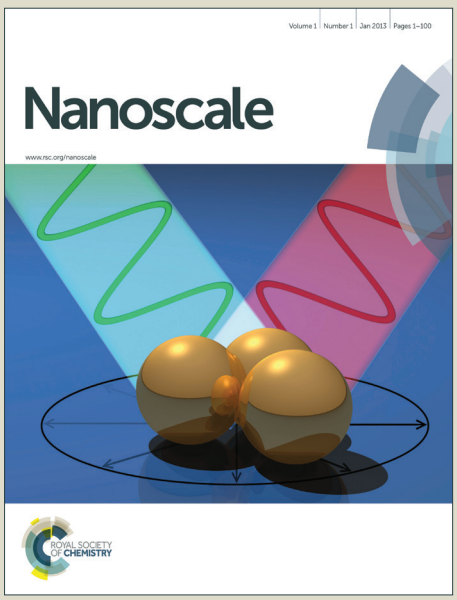

ROYAL SOCIETY OF CHEMISTRY

www.rsc.org/nanoscale

NANOSCALE

RSCPublishing

COMMUNICATION

Label-free, *in situ* SERS monitoring of individual DNA hybridization in microfluidics

Cite this: DOI: 10.1039/xoxxoooooox

Received ooth January 2012,
Accepted ooth January 2012

DOI: 10.1039/xoxxoooooox

www.rsc.org/

Ji Qi,[1] Jianbo Zeng,[1] Fusheng Zhao,[1] Steven Hsesheng Lin,[4] Balakrishnan Raja,[3] Ulrich Strych,[3] Richard C. Willson,[3,5] and Wei-Chuan Shih[1,2*]

[1]Department of Electrical and Computer Engineering, [2]Department of Biomedical Engineering, [3]Department of Chemical and Biomolecular Engineering, University of Houston, Houston TX 77204
[4]Department of Radiation Oncology, MD Anderson Cancer Center, Houston TX 7703
[5]Departamento de Biotecnología e Ingeniería de Alimentos, Tecnológico de Monterrey, Monterrey, NL 64849, Mexico
[*]Corresponding author: wshih@uh.edu

We present label-free, *in situ* monitoring of individual DNA hybridization in microfluidics. By immobilizing molecular sentinel probes on nanoporous gold disks, we demonstrate sensitivity approaching the single-molecule limit via surface-enhanced Raman scattering which provides robust signals without photobleaching for more than an hour. We further demonstrate target concentration as low as 20 pM can be detected within 10 min under diffusion-limited transport.

DNA hybridization, where two single-stranded DNA (ssDNA) molecules form duplex through non-covalent, sequence-specific interactions, is a fundamental process in biology.[1] Developing a better understanding of the kinetics and dynamic aspects of hybridization will help reveal molecular mechanisms involved in numerous biomolecular processes. To this end, sequence-specific detection of hybridization at the single-molecule level has been instrumental and gradually become a ubiquitous tool in a wide variety of biological and biomedical applications such as clinical diagnostics, biosensors, and drug development.[2] Label-free and amplification-free schemes are of particular interest because they could potentially provide *in situ* monitoring of individual hybridization events, which may lead to techniques for discriminating subtle variations due to single-base modification without stringency control or repetitive thermal cycling. To further increase experimental robustness and productivity and reduce complexity, single-step assays are highly desirable. For example, "sandwich" assay that involves multiple hybridization steps could generate highly convoluted results.

Currently, intermolecular diffusion of DNA molecules is commonly studied by fluorescence correlation spectroscopy (FCS) with an observation time limited to the diffusion time of molecules through the observation volume.[3] Single-molecule fluorescence resonance energy transfer (smFRET) and other fluorescence techniques have also been employed to study conformational changes.[4-9] Unlike most fluorescence techniques, molecular beacons (MB) provide label-free detection. However like most other fluorescence techniques, MB also suffers from rapid photobleaching which prevents prolonged observation for slow processes.[8, 10] Recently, MB probes have been immobilized on plasmonic nanoparticles to harness metal-enhanced fluorescence and achieved a limit of detection (LOD) ~500 pM.[11]

In addition to fluorescence techniques, label-free techniques for hybridization detection and biosensing include the use of localized surface plasmon resonance (LSPR),[12-14] extraordinary optical transmission,[15, 16] electrochemistry,[17, 18] circular dichroism spectroscopy[19] and mass measurements,[20] but most of these techniques cannot provide the sensitivity for single-molecule detection. Recently, carbon nanotube field-effect transistor has been demonstrated to provide label-free, single-molecule detection at relatively high target concentrations (100 nM to 1 μM).[21]

We have explored the use of surface-enhanced Raman scattering (SERS) as a reporting mechanism for molecular sensing.[22] SERS is an attractive approach for label-free multiplexed DNA/RNA detection because of its single-molecule sensitivity,[23, 24] molecular specificity,[25-27] and freedom from quenching and photobleaching.[28] These distinct advantages have led to the development of a number of SERS sensing platforms for single DNA hybridization detection, including the crescent moon structures by Lu *et al.*,[29] nanodumbbells by Lim *et al.*,[30] and Au particle-on-wire sensors by Kang *et al.*.[31] These SERS sensing platforms were able to achieve extremely high enhancement of local electromagnetic fields from "hot spots" by careful control of nanostructural assemblies.

In this paper, we present a SERS-based label-free approach capable of *in situ* monitoring of the *same* immobilized ssDNA molecules and their individual hybridization events over more than an hour. To achieve such performance, we have successfully implemented molecular sentinel (MS)[32-34] immobilized on nanoporous gold (NPG) disks[22] inside microfluidics. The microfluidic environment prevents sample drying, allows small sample volume, and permits agile fluid manipulation. MS involves the design of the complementary sequence of a target ssDNA into a stem-loop "hairpin". As shown in Fig. 1(a), the hairpin probe has a thiol group at the 5' end for robust immobilization on gold nanostructures, and a fluorophore such as cyanine 3 (Cy3) at the 3' end for SERS detection. Cy3 yields a strongly enhanced SERS signal when the probe is in the hairpin configuration; this signal decreases when the probe is hybridized with the target and moves away from the surface. MS is label-free, requires only a single hybridization step, and can be multiplexed. MS has been employed to detect breast cancer marker genes ERBB2 and RSAD2 at concentrations of 1-500 nM using colloidal silver nanoparticles.[33, 34] Detection of Ki-67 at ~1 μM has been demonstrated using a

triangular-shaped nanowire substrate, resembling a "biochip" approach,[32] which is particular attractive for point-of-care applications where minimal sample preparation is desired.

The plasmonic substrate of choice here consists of a dense monolayer of NPG disks featuring unique 3-dimensional internal porous network. The large surface area of NPG disks and hot-spots inside the nanoporous structures have contributed to an average SERS enhancement factor exceeding 10^8 and surprisingly high photothermal conversion efficiency (>50%) among metal nanoparticles of similar size with various shapes and compositions.[22, 35] We first demonstrate that the patterned NPG disk substrates provide enough SERS enhancement to enable single-molecule observation of immobilized MS probes. Second, we demonstrate that MS probes on NPG disks can be employed to perform time-lapse *in situ* monitoring of hybridization. We then show that individual DNA hybridization events can be observed and quantified as early as ~10 min after introducing 20 pM complementary target ssDNA molecules.

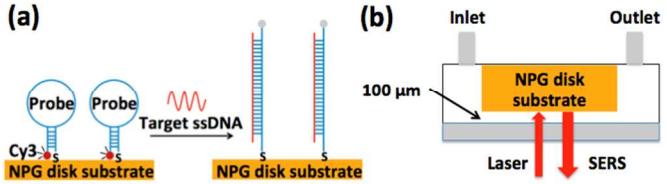

Figure 1. Schematic of MS sensing mechanism in microfluidics: (a) (left) ssDNA MS probes in a hairpin configuration are immobilized on NPG disk substrates. Intense SERS signals are observed due to the short distance between Cy3 molecules and the gold surface. Probes become straight and rigid after hybridization with target ssDNA molecules (right). The SERS signal disappears because Cy3 molecules now are about 10 nm away from the gold surface. (b) Microfluidic configuration for SERS data acquisition.

Methods

Molecular Sentinel probes and ssDNA molecules

We selected the ERBB2 gene, a critical biomarker of breast cancer, as the ssDNA target molecules. The hairpin probe consists of a complementary sequence of ERBB2 as shown in Table 1 ("ERBB2-sentinel"). Table 1 also shows the sequences of the ssDNA target ("ERBB-target") and non-complementary ssDNA ("Non-complementary control"). The underlined portion indicates the complementary stem sequences of the MS probe, and the bolded portion represents the target sequences complementary to the loop region of the MS hairpin probe. All ssDNA molecules were purchased from Integrated DNA Technologies (IDT, Coralville, IA).

Table 1. MS probe, target and non-complementary ssDNA.

ssDNA	Sequence
ERBB2-sentinel	5'-SH-CGCCAT CCACCCCCAAGACCACGACCAGC AGAATATGGCG-Cy3-3'
ERBB2-target	5'-**GTTGGCATTCTGCTGGTCGTGGTCTTGGGG GTGGTCTTTG**-3'
Non-complementary control	5'-GCCAGCGTCGAGTTGGTTTGCAGCTCCTGA-3'

NPG disks

NPG disks, 500 nm in diameter, 75 nm in thickness and 5 nm in pore size, were fabricated by a process described previously.[22] A SERS enhancement factor of ~$5*10^8$ was obtained using benzenethiol self-assembled monolayer with 785 nm laser excitation. Details of NPG disk fabrication and characterization are provided in ESI.[46]

MS probes immobilization on NPG disks and hybridization

MS hairpin probes were immobilized onto NPG disk substrates at the bottom of a PDMS microwell (2 mm diameter, 4 mm height) by incubation. 10 μL hairpin probe solutions were dispensed into the PDMS well and incubated for 40 min, following which the PDMS wells were removed and the substrates rinsed thoroughly in DI water. They were then immersed in 0.1 mM 6-mercapto-1-hexanol (MCH) for 10 minutes, followed by another DI water rinse. The substrates were then mounted inside a temperature-controlled microscope microfluidic cell culture stage (FCS2, Bioptechs) as shown in Fig. 1(b). The microscope stage was locked to ensure SERS measurements from a fixed region. A syringe pump was used to deliver target solutions of known concentration for hybridization.

To quantify and calibrate the surface density of the immobilized MS probes, we also developed an alternative technique for probe immobilization by drop casting 5 μL of probe solution directly onto the NPG disk substrate. After drying, the substrate was processed by the same rinse-MCH-rinse procedure described in the incubation approach. We then carefully inspected the spot area (~3 mm diameter) under an optical microscope and a Raman microscope to verify the coating distribution, allowing us to estimate the surface density of MS probes. More details are provided in ESI.[46]

SERS Measurement

SERS measurements were carried out using an line-scan Raman microscopy system with 785 nm excitation.[36] The laser was focused on the sample as a line with a length of 133 μm and width of 1 μm. Raman scattered photons from the entire line were imaged with 60X magnification onto the entrance slit of a dispersive spectrograph coupled to a charge coupled device (CCD) camera. The spatial and spectral resolution were ~1 μm and ~8 cm^{-1}, respectively. The acquisition time for each CCD frame was 10 s at a laser power density of 0.1 mW/μm^2. Full-frame data of dimension 133 (spatial) x 1340 (λ) were collected, equivalent to 133 "point-spectra", each from a 1-μm^2 spot. A "line-spectrum" was obtained by averaging the 133 point-spectra in one CCD frame.

Results

SERS detection of immobilized MS probes

Figure 2 shows SERS line-spectra from different concentrations of ERBB2-sentinel probes on NPG disk substrates by incubation (500 pM–5 nM) and drop cast (100 pM), respectively. Each line-spectrum is an average of 133 point-spectra from a single CCD frame (133 (spatial) x 1340 (λ)). The baselines were approximated by a 5th order polynomial and removed.[37] The major peaks at 1197 cm^{-1}, 1393 cm^{-1}, 1468 cm^{-1} and 1590 cm^{-1} were assigned to Cy3.[25] The presence of these major peaks indicates that the probe molecules were in their hairpin configuration, with the 3'-Cy3 near the gold surface. The Raman band at 1078 cm^{-1} (marked with an asterisk) is assigned to MCH. In the following experiments, we use the Cy3 peak height at 1197 cm^{-1} as the SERS intensity indicator. The immobilized probe density of drop cast onto NPG disk substrates was estimated from the number of probe molecules pipetted onto the NPG disk surface. Drop cast of 5 μL 100 pM probe solution resulted in about 2 probe molecules/μm^2 after the rinse-MCH-rinse protocol described previously. The probe density on NPG disk substrates using the incubation method was estimated by calibrating against the SERS intensity obtained from drop cast substrates. More details on the quantification are provided in ESI.[46]

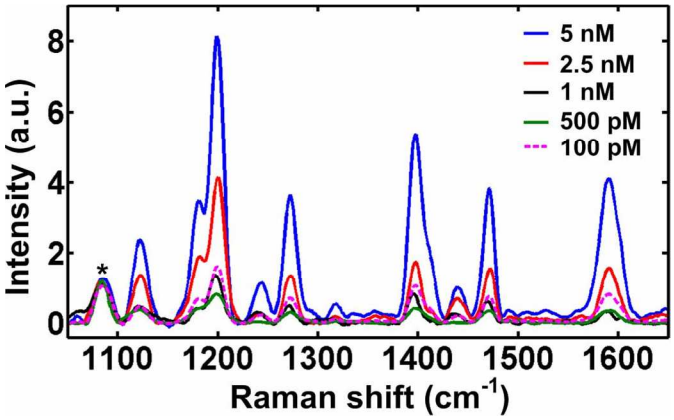

Figure 2. SERS spectra of the MS probes on NPG disk substrates by incubation (500 pM–5 nM) and drop cast (100 pM) immobilization protocols.

In situ monitoring of DNA hybridization with varying target ssDNA concentrations using incubation for probe immobilization

In the first series of experiments, we employed the incubation technique to immobilize 5 nM sentinel probe solutions, along with target concentrations from 5 to 20 nM. SERS monitoring began after the substrate was mounted into the microscope microfluidic chamber with 10 – 15 min acquisition intervals. Figure 3(a) shows the Cy3 intensities at 1197 cm^{-1} from the line-spectra after introducing the target ssDNA molecules. Three representative line-spectra from the hybridization and the plateau phases of this experiment are shown in the upper-right corner.

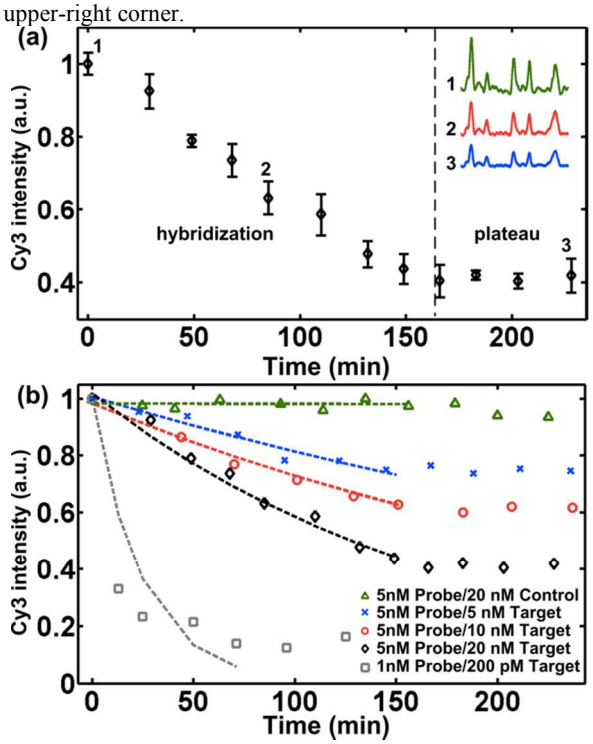

Figure 3. *In situ* hybridization monitoring using SERS line-spectra: (a) 5 nM MS probe hybridization with 20 nM target, (b) 5 nM MS probe hybridization with 5, 10, 20 nM target (cross, circle and diamond) and 20 nM non-complementary ssDNA (triangle); 1 nM MS probe hybridization with 200 pM target (square). Dashed curves are the exponential fits for the hybridization phase.

As shown in Fig. 3(a), the SERS intensity began to decrease due to hybridization after introducing the 20 nM target solution. The SERS intensity reached a plateau phase at ~170 min, indicating the endpoint of hybridization. Measurements over another 40 min indicated that no further hybridization occurred. We observed a 60% SERS intensity decrease from the 5 nM/20 nM (probe/target) experiment, i.e., 60% of the immobilized probes reacted with the target ssDNA molecules. A plausible explanation for the incomplete consumption of all immobilized probes is inefficient mass transfer of target ssDNA molecules to the NPG disk surface. According to the adsorption kinetics model of biomolecules[38], only a tiny fraction of target ssDNA molecules were able to react with probes in the current diffusion-limited configuration.

Figure 3(b) shows the hybridization and plateau phase of experiments with different target concentrations and non-complementary ssDNA molecules. The dashed curves are exponential fits. We observed a greater time constant at higher target concentrations, suggesting that target concentration can be determined by monitoring the decrease rate of Cy3 intensity. Alternatively, the final intensity value was also indicative of the target concentration. In the negative control experiment, 20 nM non-complementary ssDNA molecules did not cause a statistically meaningful SERS intensity change (±5%). Since the non-complementary ssDNA molecules could not hybridize with the ERBB-sentinel probe, the Cy3 label remained close to the gold surface, thus maintaining a strong and stable SERS signal. Furthermore, the stable SERS signal indicated that there was no photobleaching during experiments and the probe immobilization was robust. We thus attributed any signal decrease after adding target ssDNA molecules to hybridization. To explore the detection limit in terms of number of target DNA molecules for our sensor, we reduced the concentration of the sentinel probe to 1 nM for immobilization by incubation, resulting in a probe density of about 2 molecules/μm^2. The Cy3 SERS intensity time trace after adding a 200 pM target solution is displayed as squares in Fig. 3(b). The Cy3 intensity decreased significantly within the first 13 min after the introduction of target and reached a plateau phase 90 min later. About 80% overall intensity decrease was observed.

Instead of the overall time trace extracted from the line-spectra as shown in Fig. 3(a) and (b), we next study individual time traces from point-spectra by taking advantage of the spatial resolution of the line-scan Raman system. Ideally, there were 133 time traces using the point-spectrum, each from a 1-μm^2 spot. Since the probe density was estimated to be about 2 molecules/μm^2 for substrates incubated in 1 nM MS probe solutions, and we observed an average SERS intensities of 200 CCD counts, we interpret each 100 CCD counts as a single MS probe. Equivalently, each intensity decrease of 100 CCD counts during hybridization is attributed to a single hybridization event. We consequently use an interval of 100 CCD counts between centers of bins in the following statistical analyses.

Figure 4 displays the histograms of immobilized probe count and hybridization event count by studying individual time traces. The point-spectra showing extremely high SERS intensities at different peak locations different from Cy3, likely from impurities in the solution, were excluded from the statistical study. The number of time traces involved in the statistical analyses are 106, 101, 112 and 93 for probe/target pairs of 5 nM/5 nM, 5 nM/10 nM, 5 nM/20 nM and 1 nM/200 pM, respectively. The blue bars in Fig. 4 represent the frequency of the immobilized probe count on 1-μm^2 NPG disk surface before hybridization. We found that these histograms (blue bars) can be better fit by Poisson distribution than Gaussian with an average of 10 and 2 (shown as magenta diamonds) for substrates incubated in 5 nM and 1 nM probe solutions, respectively. This agrees well with our previous interpretation that 100 CCD counts represent a single probe.

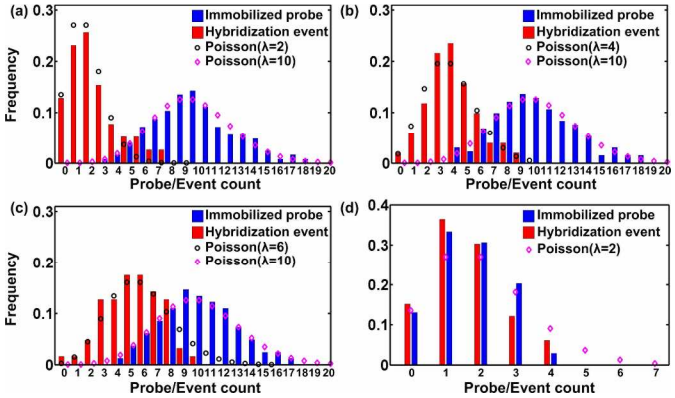

Figure 4. Statistical analysis of individual time traces at probe/target concentrations of (a) 5 nM/5 nM, (b) 5 nM/10 nM, (c) 5 nM/20 nM and (d) 1 nM/200 pM. See text for details.

The red bars represent the frequency of hybridization event count. We observe more hybridization events at higher target concentrations in 5 nM incubation experiments, which is consistent with the intensity time traces in Fig. 3(b). Similarly, the histograms of hybridization event count can be better fit by Poisson distribution (black circle in Fig. 4(a)-(c), magenta diamond in Fig. 4(d)) with averages of 2, 4, 6, and 2 for 5 nM, 10 nM, 20 nM and 200 pM target concentrations, respectively. In other words, 2, 4, 6, and 2 hybridization events were observed on average for 5 nM, 10 nM, 20 nM, and 200 pM target solutions, respectively.

In situ monitoring of DNA hybridization with 20 pM target ssDNA concentration using drop cast for probe immobilization

In this series of experiments, we employed drop cast as an alternative approach for probe immobilization. As discussed in the ESI,[46] the probe surface density by drop cast of 100 pM probe solutions is equivalent to that from incubating in 1 nM solutions, with both method resulting in about 2 probe molecules/μm^2 before hybridization. A protocol identical to the previous experiment was followed except that a 20 pM target solution was used. As shown in Fig. 5(a), the line-spectra SERS intensity decreased substantially after the 20 pM target was introduced with the earliest detection at 10 min. Figure 5(b), (c) and (d) show the full-frame SERS images just before adding the target, during hybridization and at the last measurements (time points 1, 2 and 3 in Fig. 5(a)), respectively. The major peaks from Cy3 clearly visible in Fig. 5(b) diminished significantly in Fig. 5(d). The overall Cy3 intensity decrease was ~80% at 90 min after introducing the target. As shown in Fig. 5(f), the histogram (blue bars) of the immobilized probe count agrees well with Poisson distribution with an average of 2. A similar distribution is observed in the histogram of hybridization event count as discussed later. Analyzing the point-spectra from 64 spots, four representative intensity patterns are observed and shown in Fig. 5(e). Trace 1 (red), Trace 2 (blue) and Trace 4 (black) exhibit a single-step intensity drop of 100, 200, and 400 CCD counts, respectively. Trace 3 (magenta) exhibits a two-step intensity drop with 200 CCD counts in the first step and then 100 in the second. The observation of quantized intensity decreases in individual time traces provide further support that individual hybridization events were observed. In the experiment using incubation in 1 nM probe solution, we also observed similar quantized intensity decreases in individual time traces. The intensity patterns 1-4 correspond to 1-4 hybridization events (red bars) taking place on the 1-μm^2 spots.

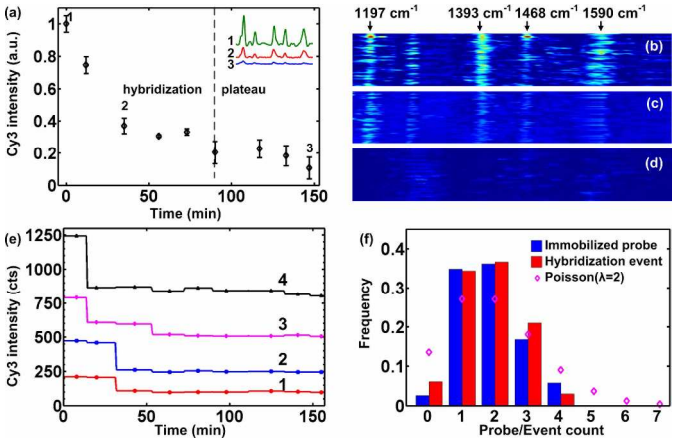

Figure 5. (a) Overall Cy3 intensity trace with 20 pM target DNA; SERS image at (b) t=0 min, (c) t=40 min and (d) t= 150 min; the horizontal axis represents wavenumbers. Each row in the SERS image is a single point-spectrum. The major bands of Cy3 are labeled; (e) representative intensity patterns 1-4 corresponding to the hybridization counts 1-4 in Fig. 5(f) (red bars); (f) histogram analysis of individual time traces from 64 1-μm^2 spots.

Using the representative intensity patterns shown in Fig. 5(e), we have performed a statistical analysis of 64 individual hybridization time traces with results shown in Fig. 5(f). As mentioned earlier, the blue bars represent the statistics of immobilized MS probes. The red bars represent total hybridization events during the hybridization phase over individual 1-μm^2 spots. Both histograms can be better fit with a Poisson distribution of λ=2 (diamond in Fig. 5(f)) than with a Gaussian distribution. Although there has been debate on whether to expect a Poisson distribution of SERS intensities at ultra-low concentrations[39-41], here it is only employed to provide additional insight into our results, not to justify the claim of single-molecule detection. In addition, the enhancements of SERS signals from the NPG disk substrates were uniform across a large area (at least 100 ×100 μm^2).[22] Therefore, our measurements of SERS intensities are reliable, and not affected by the factors summarized in Ref. 39 that could potentially invalidate interpreting Poisson statistics as single-molecule events.

Next we discuss the implications of our results within the context of microfluidic sensors, where the static or laminar flow nature poses significant challenges for achieving low LOD. Unlike sensors implemented in un-restricted fluidic environments, e.g., beaker, where active mixing is readily available, the transport of target molecules to the sensing surface largely depends on diffusion in microchannels. Compared with several recently published label-free microfluidic sensors, our demonstrated LOD (20 pM) is respectable even without any attempt of optimization.[11, 42-44] After all, the technique does have sensitivity approaching single-molecule. So a future challenge appears to be implementing efficient means for bringing target molecules to the MS probes for hybridization. For example, it is quite possible to lower the LOD with the help of active concentrating mechanisms such as dielectrophoresis.[45]

Conclusion

We have developed a label-free technique to *in situ* monitor DNA hybridization using molecular sentinel probes immobilized on patterned nanoporous gold disk SERS substrates by taking advantage of the ultrahigh SERS sensitivity of these novel substrates. In addition, we were able to detect the onset of hybridization events within ~10 min after introducing 20 pM target ssDNA molecules. Given sensitivity approaching the single-molecule limit, robust SERS signals, and simple detection system,

this approach could find potential applications in time-lapsed monitoring of DNA interactions and point-of-care applications.

R.C.W. acknowledges NSF (CMMI-0900743), the Welch Foundation (E-1264), and Huffington-Woestemeyer Professorship. W.C.S. acknowledges NSF CAREER Award (CBET-1151154), NASA Early CAREER Faculty Grant (NNX12AQ44G), and Gulf of Mexico Research Initiative (GoMRI-030).

Electronic Supplementary Information (ESI) available: NPG disk fabrication and characterization, probe density estimation, and hybridization temperature. See DOI: 10.1039/c000000x/

1. Y. D. Yin and X. S. Zhao, *Accounts Chem Res*, 2011, **44**, 1172-1181.
2. A. Sassolas, B. D. Leca-Bouvier and L. J. Blum, *Chemical Reviews*, 2008, **108**, 109-139.
3. M. Kinjo and R. Rigler, *Nucleic Acids Research*, 1995, **23**, 1795-1799.
4. X. W. Zhuang, L. E. Bartley, H. P. Babcock, R. Russell, T. J. Ha, D. Herschlag and S. Chu, *Science*, 2000, **288**, 2048-+.
5. B. S. Gaylord, A. J. Heeger and G. C. Bazan, *P Natl Acad Sci USA*, 2002, **99**, 10954-10957.
6. O. P. Kallioniemi, A. Kallioniemi, W. Kurisu, A. Thor, L. C. Chen, H. S. Smith, F. M. Waldman, D. Pinkel and J. W. Gray, *P Natl Acad Sci USA*, 1992, **89**, 5321-5325.
7. D. J. Lockhart, H. L. Dong, M. C. Byrne, M. T. Follettie, M. V. Gallo, M. S. Chee, M. Mittmann, C. W. Wang, M. Kobayashi, H. Horton and E. L. Brown, *Nat Biotechnol*, 1996, **14**, 1675-1680.
8. S. Tyagi and F. R. Kramer, *Nat Biotechnol*, 1996, **14**, 303-308.
9. H. C. Yeh, J. Sharma, J. J. Han, J. S. Martinez and J. H. Werner, *Nano Lett*, 2010, **10**, 3106-3110.
10. G. Yao, X. H. Fang, H. Yokota, T. Yanagida and W. H. Tan, *Chemistry-a European Journal*, 2003, **9**, 5686-5692.
11. H. I. Peng, C. M. Strohsahl and B. L. Miller, *Lab on a chip*, 2012, **12**, 1089-1093.
12. Y. Chen, K. Munechika and D. S. Ginger, *Nano Lett*, 2007, **7**, 690-696.
13. C. Sonnichsen, B. M. Reinhard, J. Liphardt and A. P. Alivisatos, *Nat Biotechnol*, 2005, **23**, 741-745.
14. Y. Shen, J. H. Zhou, T. R. Liu, Y. T. Tao, R. B. Jiang, M. X. Liu, G. H. Xiao, J. H. Zhu, Z. K. Zhou, X. H. Wang, C. J. Jin and J. F. Wang, *Nat Commun*, 2013, **4**.
15. R. Gordon, D. Sinton, K. L. Kavanagh and A. G. Brolo, *Accounts Chem Res*, 2008, **41**, 1049-1057.
16. A. A. Yanik, M. Huang, O. Kamohara, A. Artar, T. W. Geisbert, J. H. Connor and H. Altug, *Nano Lett*, 2010, **10**, 4962-4969.
17. T. G. Drummond, M. G. Hill and J. K. Barton, *Nat Biotechnol*, 2003, **21**, 1192-1199.
18. J. Wang, G. D. Liu and A. Merkoci, *J Am Chem Soc*, 2003, **125**, 3214-3215.
19. W. Ma, H. Kuang, L. G. Xu, L. Ding, C. L. Xu, L. B. Wang and N. A. Kotov, *Nat Commun*, 2013, **4**.
20. P. Ross, L. Hall, I. Smirnov and L. Haff, *Nat Biotechnol*, 1998, **16**, 1347-1351.
21. S. Sorgenfrei, C. Y. Chiu, R. L. Gonzalez, Y. J. Yu, P. Kim, C. Nuckolls and K. L. Shepard, *Nat Nanotechnol*, 2011, **6**, 125-131.
22. J. Qi, P. Motwani, M. Gheewala, C. Brennan, J. C. Wolfe and W.-C. Shih, *Nanoscale*, 2013, **5**, 4105-4109.
23. S. M. Nie and S. R. Emery, *Science*, 1997, **275**, 1102-1106.
24. K. Kneipp, Y. Wang, H. Kneipp, L. T. Perelman, I. Itzkan, R. Dasari and M. S. Feld, *Phys Rev Lett*, 1997, **78**, 1667-1670.
25. Y. C. Cao, R. Jin and C. A. Mirkin, *Science*, 2002, **297**, 1536-1540.
26. C. L. Haynes, A. D. McFarland and R. P. Van Duyne, *Anal Chem*, 2005, **77**, 338A-346A.
27. H. Im, K. C. Bantz, N. C. Lindquist, C. L. Haynes and S. H. Oh, *Nano Lett*, 2010, **10**, 2231-2236.
28. W. E. Doering and S. M. Nie, *Anal Chem*, 2003, **75**, 6171-6176.
29. Y. Lu, G. L. Liu, J. Kim, Y. X. Mejia and L. P. Lee, *Nano Lett*, 2005, **5**, 119-124.
30. D. K. Lim, K. S. Jeon, H. M. Kim, J. M. Nam and Y. D. Suh, *Nature materials*, 2010, **9**, 60-67.
31. T. Kang, S. M. Yoo, I. Yoon, S. Y. Lee and B. Kim, *Nano Lett*, 2010, **10**, 1189-1193.
32. H. N. Wang, A. Dhawan, Y. Du, D. Batchelor, D. N. Leonard, V. Misra and T. Vo-Dinh, *Physical chemistry chemical physics : PCCP*, 2013, **15**, 6008-6015.
33. H. N. Wang, A. M. Fales, A. K. Zaas, C. W. Woods, T. Burke, G. S. Ginsburg and T. Vo-Dinh, *Analytica chimica acta*, 2013, **786**, 153-158.
34. H. N. Wang and T. Vo-Dinh, *Nanotechnology*, 2009, **20**, 065101.
35. G. M. Santos, F. S. Zhao, J. B. Zeng and W. C. Shih, *Nanoscale*, 2014, DOI: 10.1039/C4NR00017J.
36. J. Qi and W. C. Shih, *Applied Optics*, 2014, 53, 2881-2885.
37. J. Qi, J. Li and W.-C. Shih, *Biomedical Optics Express*, 2013, **4**, 2376-2382.
38. K. C. Dee, D. A. Puleo and R. Bizios, in *An Introduction To Tissue-Biomaterial Interactions*, John Wiley & Sons, Inc., 2003, pp. 37-52.
39. P. G. Etchegoin, M. Meyer and E. C. Le Ru, *Physical Chemistry Chemical Physics*, 2007, **9**, 3006-3010.
40. J. P. Camden, J. A. Dieringer, J. Zhao and R. P. Van Duyne, *Accounts Chem Res*, 2008, **41**, 1653-1661.
41. J. Kneipp, H. Kneipp and K. Kneipp, *Chem Soc Rev*, 2008, **37**, 1052-1060.
42. J. Wang, D. Onoshima, M. Aki, Y. Okamoto, N. Kaji, M. Tokeshi and Y. Baba, *Anal Chem*, 2011, **83**, 3528-3532.
43. P. Lin, X. T. Luo, I. M. Hsing and F. Yan, *Advanced Materials*, 2011, **23**, 4035-+.
44. S. W. Dutse and N. A. Yusof, *Sensors*, 2011, **11**, 5754-5768.
45. A. Barik, L. M. Otto, D. Yoo, J. Jose, T. W. Johnson and S.-H. Oh, *Nano Lett*, 2014, **14**, 2006-2012.
46. ESI: NPG disk fabrication and characterization, Probe density estimation, and hybridization temperature.